

200906014A

別紙 1

研究報告書表紙

厚生労働科学研究費補助金

再生医療実用化研究事業

培養細胞または幹細胞を用いた再生ヒト角膜内皮移植の実用化に関する研究

平成 21 年度 総括研究報告書

研究代表者 三村 達哉

平成 22 (2010) 年 5 月

研究報告書目次

目 次

I. 総括研究報告		
培養細胞または幹細胞を用いた再生ヒト角膜内皮移植の実用化に関する研究	-----	1
三村 達哉		
II. 研究成果の刊行に関する一覧表	-----	3
III. 研究成果の刊行物・別刷	-----	4

## I. 総括研究報告

厚生労働科学研究費補助金（再生医療実用化研究事業）  
（総括）研究報告書

## 培養細胞または幹細胞を用いた再生ヒト角膜内皮移植の実用化に関する研究

研究代表者 三村達哉 虎の門病院眼科 医師・研究員

## 研究要旨

角膜ドナー不足を解消するために、再生した角膜内皮により角膜混濁を治療することを目的としている。培養ヒト角膜内皮細胞あるいは、ヒト角膜組織幹細胞を用いて、角膜内皮を再生した。再生内皮は生体内同様の機能を有し、動物眼に移植することにより水疱性角膜症の治療に有効であった。

**A. 研究目的：**本邦の角膜移植手術におけるドナー角膜不足は深刻であり、ドナー角膜を必要としない、人工角膜の開発に期待がかかっている。ヒト角膜は角膜上皮、実質、内皮にわかれ、その中で角膜内皮細胞は角膜透明性維持に最も重要であるが、生体内では増殖能を失っているために、加齢に伴った角膜内皮細胞の減少が角膜透明性減少の原因となっている。我々は角膜再生を目的として、細胞外基質、培養細胞あるいは生体幹細胞を用いた角膜上皮、実質、内皮の再生について精力的に研究を行っている。角膜上皮混濁に対しては、自己の健常部分より採取して培養した角膜上皮細胞、結膜上皮細胞、あるいは口腔粘膜上皮細胞のシートによる眼表面再生医療を既に行っている。しかし、角膜混濁を来す症例は全層が障害されていることが大半で、その多くは角膜内皮細胞の障害による不可逆的な水疱性角膜症である。本研究では、角膜内皮に焦点をあて、培養ヒト角膜内皮細胞を用いた角膜内皮シートあるいは幹細胞を移植することにより混濁した角膜を透明にする治療の実用化を目的としている。

**B. 研究方法：**

## 研究計画および方法

**角膜幹細胞を用いた再構築角膜**

- ① 再構築内皮シートの移植実験：臨床応用に向けて動物眼への移植実験を行う。
- ② 移植法：内皮幹細胞の移植法ならびに、移植用器具を開発する。

角膜内皮より選択的に幹細胞を採取し、生体外で培養し、移植を行う。一般的に、術後 allo 移植よりは auto 移植の方が、拒絶反応を起こしにくいいため、自己細胞の移植が理想となる。また分化した培養細胞を移植しても、術後生体内での増殖能は期待できない。そこで、患者の健常眼の片眼から自己の幹細胞を選択的に採取して、罹患眼に移植する方法は、移植後も細胞は増殖する可能性があり、細胞供給源となる可能性がある。拒絶反応抑制と移植後の細胞供給源の利点を兼ね備えた自己幹細胞移植についても、検討した。

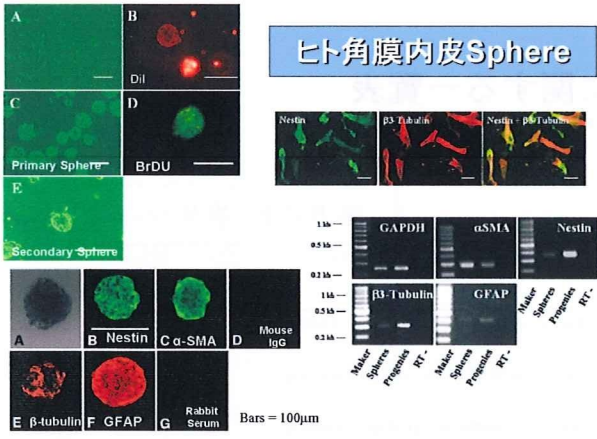
**(倫理面への配慮)**

すべての研究は東京大学倫理委員会の承認を得て行う。角膜幹細胞を用いた人工角膜の人への移植を前提とした研究であるため、倫理委員会の指針、動物実験の対する指針、および研究に関与するあらゆる倫理指針を遵守する。動物の取り扱いは、苦痛を伴うものは必ず全身麻酔下に行い、両眼が失われる可能性のある場合は片眼のみに処置を行う。全ての実験において動物は the Association for Research in Vision and Ophthalmology の規約および、実験動物の飼養及び保管等に関する基準（総理府）に従って扱う。人を扱う研究では、ヘルシンキ宣言（世界医師会総会 World Medical Assembly）の勧告に従って行う。また遺伝子解析はヒトゲノム・遺伝子解析研究に関する倫理指針（文部科学省、厚生労働省、経済産業省）に従い、幹細胞の取り扱いはヒト幹細胞を用いた臨床研究に関する指針（厚生労働省）を遵守する。患者を対象とする臨床試験においては十分な説明をした後、文書による同意を得てから行う（インフォームド・コンセント）。

**C. 研究結果：**

内皮層より選択的に採取した組織幹細胞は神経未分化マーカーNestinを発現した。また分化誘導培地で培養して得られた細胞は角膜内皮様の正六角形細胞に分化し、RT-PCR法にて内皮細胞と同様の遺伝子発現パターンを示した。織幹細胞を用いて再構築した内皮シートは十分な強度を持ち、移植可能であった。

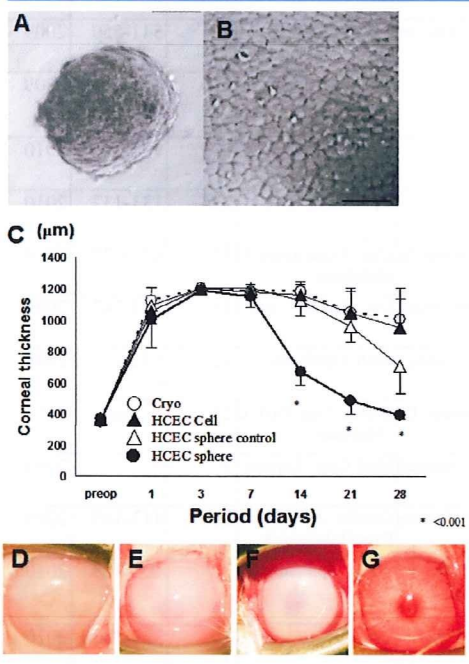
内皮細胞を除去することにより角膜が混濁した家兎水疱性角膜症モデルに角膜内皮組織幹細胞を移植したところ、透明性および角膜厚は正常に回復した。経過観察中、術後拒絶反応は認められず、角膜透明性を維持した。



**ヒト角膜内皮Sphere**

浮遊培養法（スフェア法）によるヒト角膜内皮前駆細胞の採取。ドナーからのヒト角膜内皮細胞より1次および二次 sphere が形成される。sphere は BRDU の

**ヒト角膜内皮細胞由来体性幹細胞の移植**



継代5代目の培養HCECよりニューロスフェア法により角膜内皮体性幹細胞を選択的に採取し(A), 内皮障害のある家兎に移植した。培養細胞より得られたスフェアを培養皿上で再培養すると、角膜内皮特有の正六角形の形態を示している(B)。培養HCEC由来の幹細胞または培養HCECを次の4群に分けて、角膜内皮細胞を障害した家兎に移植した。Negative control 群(角膜内皮障害後、無治療群, n=6), HCEC 群(角膜内皮障害後、培養HCECを前房内に注入し、24時間うつぶせにした群, n=6), Sphere-face-up 群(角膜内皮障害後、HCEC スフェアを前房内に注入し、体位を自由にさせた群, n=6), Sphere-face-down 群(角膜内皮障害後、HCEC スフェアを前房内に注入し、24時間うつぶせにした群, n=6)。C: 術後角膜厚(縦軸)。術後経過(横軸)。Sphere-face-down 群の角膜厚は3日、7日、14日、21日、28日目において他のコントロールと比較して有意に低下している(p<0.001)。術後前眼部を観察すると Negative control 群(D), HCEC 群(E), Sphere-face-up 群(F)では角膜混濁が強いが、Sphere-face-down 群では角膜は透明で実質浮腫は認められない(G)。

D. 考察: 培養角膜内皮細胞および角膜内皮組織幹細胞による再構築角膜はの移植後長期成績を動物眼で今後検討する必要があるが、今後の臨床応用に対して大いに期待できる方法であると考えられた。

E. 結論 再生内皮は生体内同様の機能を有し、動物眼に移植することにより水疱性角膜症の治療に有効であった。

F. 健康危険情報 本研究の結果により、健康に及ぼす危険事項は確認できなかった。

**G. 研究発表**

1. 論文発表 2009年以降 英文 29報

1. Noma H, **Mimura T.** et al. BMC Ophthalmol. 2010;10:11.
2. Honda N, **Mimura T.** et al. Arch Ophthalmol. 2010;128:466-71.
3. Noma H, **Mimura T.** et al. Graefes Arch Clin Exp Ophthalmol. 2010 Mar 23.
4. Fukuoka S, **Mimura T.** et al. Cornea. 2010;29:528-30.
5. Tsuji H, **Mimura T.** et al. Arch Ophthalmol. 2010;128:258-9.
6. Tsuji H, **Mimura T.** et al. Br J Ophthalmol. 2010;94:261-2.
7. Azar DT, **Mimura T.** et al. Cornea. 2010;29:321-30.
8. Noma H, **Mimura T.** et al. Eur J Ophthalmol. 2010;20:402-9.
9. Noma H, **Mimura T.** et al. Graefes Arch Clin Exp Ophthalmol. 2010;248:443-5.
10. Tatsugawa M, **Mimura T.** et al. J Med Case Reports. 2009;3:104.
11. **Mimura T.** et al. Eng Part C Methods. 2009 Oct 23.
12. Honda N, **Mimura T.** et al. Arch Ophthalmol. 2009;127:1321-6.
13. **Mimura T.** et al. Eye Contact Lens. 2009;35:345-7.
14. **Mimura T.** et al. Clin Experiment Ophthalmol. 2009;37:670-7.
15. **Mimura T.** et al. Ophthalmologica. 2010;224:133-7.
16. **Mimura T.** et al. Ophthalmologica. 2010;224:90-5.
17. **Mimura T.** et al. Ophthalmology. 2009;116:1880-6.
18. **Mimura T.** et al. J Vasc Res. 2009;46:541-50.
19. **Mimura T.** et al. Acta Ophthalmol. 2009 Jun 26.
20. **Mimura T.** et al. Am J Ophthalmol. 2009;148:20-5.
21. Araki F, **Mimura T.** et al. Br J Ophthalmol. 2009;93:554-6.
22. Noma H, **Mimura T.** et al. Br J Ophthalmol. 2009;93:630-3.
23. Noma H, **Mimura T.** et al. Ophthalmology. 2009;116:87-93.
24. Funatsu H, **Mimura T.** et al. Ophthalmology. 2009;116:73-9.
25. Yamasaki M, **Mimura T.** et al. Int Ophthalmol. 2009;29:161-7.
26. **Mimura T.** et al. Am J Ophthalmol. 2009;147:171-177.
27. Funatsu H, **Mimura T.** et al. Acta Ophthalmol. 2009;87:501-5.
28. Noma H, **Mimura T.** et al. Acta Ophthalmol. 2009;87:638-42.
29. **Mimura T.** et al. Eye (Lond). 2009;23:63-6.

**2. 学会発表**

- ① 第113回日本眼科学会総会 7演題発表
- ② 第62回日本臨床眼科学会 4演題発表
- ③ 第34回角膜カンファレンス 2演題発表
- ④ TERMIS, 2009 国際再生医療学会 (Seoul) 1演題発表
- ⑤ 第114回日本眼科学会総会 2演題発表
- ⑥ ARVO2010 (USA フロリダ) 1演題発表

**H. 知的財産権の出願・登録状況**

1. 特許取得 国内 3 国際特許 1
2. 実用新案登録 なし
3. その他・賞罰  
**三村達哉** 第33回角膜カンファレンス・第25回日本角膜移植学会 内田賞 平成21年

## II. 研究成果の刊行に関する一覧表

雑誌

発表者氏名	論文タイトル名	発表誌名	巻号	ページ	出版年
Mimura T, Mimura Y, Arimoto A, Amano S, Yamagami S, Funatsu H, Usui T, Noma H, Honda N, Okamoto S.	Relationship between refraction and allergic conjunctivitis.	Eye (Lond)	23	63-66	2009
Mimura T, Yamagami S, Usui T, Funatsu H, Mimura Y, Noma H, Honda N, Amano S.	Changes of conjunctivochalasis with age in a hospital-based study.	Am J Ophthalmol.	147	171-177	2009
Funatsu H, Noma H, Mimura T, Eguchi S, Hori S.	Association of vitreous inflammatory factors with diabetic macular edema.	Ophthalmology	116	73-9.	2009
Noma H, Funatsu H, Mimura T, Harino S, Hori S.	Vitreous levels of interleukin-6 and vascular endothelial growth factor in macular edema with central retinal vein occlusion.	Ophthalmology	116	87-93	2009
Araki F, Mimura T, Fukuoka S, Tsuji H, Izutsu K, Yamamoto H, Takazawa Y, Kojima T.	Primary orbital lymphomatoid granulomatosis.	Br J Ophthalmol.	93	554-556	2009
Noma H, Funatsu H, Sakata K, Harino S, Nagaoka T, Mimura T, Sone T, Hori S.	Macular Microcirculation and Macular Oedema in Branch Retinal Vein Occlusion.	Br J Ophthalmol.	93	630-633	2009
Mimura T, Usui T, Yamamoto H, Yamagami S, Funatsu H, Noma H, Honda N, Fukuoka S, Amano S.	Conjunctivochalasis and contact lenses.	Am J Ophthalmol.	148	20-25	2009
Noma H, Funatsu H, Mimura T, Harino S, Sone T, Hori S.	Increase of vascular endothelial growth factor and interleukin-6 in the aqueous humour of patients with macular oedema and central retinal vein occlusion.	Acta Ophthalmologica	26	In press	2009
Mimura T, Han KY, Onguchi T, Chang JH, Kim TI, Kojima T, Zhou Z, Azar DT.	MT1-MMP-mediated cleavage of decorin in corneal angiogenesis.	J Vasc Res.	46	541-550	2009
Mimura T, Usui T, Yamagami S, Funatsu H, Noma H, Honda N, Fukuoka S, Shirakawa R, Hotta H, Amano S.	Subconjunctival hemorrhage and conjunctivochalasis.	Ophthalmology	116	1880-1886	2009
Mimura T, Yamagami S, Usui T, Funatsu H, Noma H, Honda N, Fukuoka S, Hotta H, Amano S.	Location and extent of subconjunctival hemorrhage.	Ophthalmologica	224	90-95	2010
Mimura T, Usui T, Yamagami S, Funatsu H, Noma H, Honda N, Amano S.	Recent causes of subconjunctival hemorrhage.	Ophthalmologica	224	133-137	2010
Mimura T, Yamagami S, Usui T, Funatsu H, Noma H, Honda N, Amano S.	Relationship between myopia and allergen-specific serum IgE levels in patients with allergic conjunctivitis.	Clin Experiment Ophthalmol	37	670-677	2009
Mimura T, Fujimura S, Yamagami S, Usui T, Honda N, Shirakawa R, Fukuoka S, Amano S.	Severe hyperopic shift and irregular astigmatism after radial keratotomy.	Eye Contact Lens.	35	345-347	2009
Honda N, Mimura T, Usui T, Amano S.	Descemet stripping automated endothelial keratoplasty using cultured corneal endothelial cells in a rabbit model.	Arch Ophthalmol	127	1321-1326	2009
Mimura T, Yamagami S, Yokoo S, Usui T, Amano S.	Selective Isolation of Young Cells from Human Corneal Endothelium by the Sphere-Forming Assay.	Tissue Eng Part C Methods	23	In press	2009
Tatsugawa M, Noma H, Mimura T, Funatsu H.	Unusual orbital lymphoma undetectable by magnetic resonance imaging: a case report.	Med Case Reports	3	3	2009
Noma H, Funatsu H, Sakata K, Mimura T, Hori S.	Macular microcirculation before and after vitrectomy for macular edema with branch retinal vein occlusion.	Graefes Arch Clin Exp Ophthalmol	248	443-445	2009
Noma H, Funatsu H, Mimura T, Harino S, Hori S.	Aqueous humor levels of vasoactive molecules correlate with vitreous levels and macular edema in central retinal vein occlusion.	Eur J Ophthalmol	20	402-409	2010
Azar DT, Casanova FH, Mimura T, Jain S, Zhou Z, Han KY, Chang JH.	Corneal epithelial MT1-MMP inhibits vascular endothelial cell proliferation and migration.	Cornea	29	321-330	2010
Tsuji H, Kanda H, Kashiwagi H, Mimura T.	Primary epithelioid haemangi endothelioma of the eyelid.	Br J Ophthalmol	94	261-262	2010
Tsuji H, Tamura M, Yokoyama M, Takeuchi K, Mimura T.	Ocular involvement by Epstein-Barr virus-positive diffuse large B-cell lymphoma of the elderly: a new disease entity in the world health organization classification.	Arch Ophthalmol.	128	258-259	2010
Fukuoka S, Honda N, Ono K, Mimura T, Usui T, Amano S.	Extended long-term results of penetrating keratoplasty for keratoconus.	Cornea	29	528-530	2010
Noma H, Funatsu H, Sakata K, Mimura T, Hori S.	Association between macular microcirculation and soluble intercellular adhesion molecule-1 in patients with macular edema and retinal vein occlusion.	Graefes Arch Clin Exp Ophthalmol.	23	In press	2010
Honda N, Miyai T, Nejima R, Miyata K, Mimura T, Usui T, Aihara M, Araie M, Amano S.	Effect of latanoprost on the expression of matrix metalloproteinases and tissue inhibitor of metalloproteinase 1 on the ocular surface.	Arch Ophthalmol.	128	466-471	2010
Noma H, Funatsu H, Mimura T, Eguchi S, Shimada K.	Visual acuity and foveal thickness after vitrectomy for macular edema associated with branch retinal vein occlusion: a case series.	BMC Ophthalmol	10	11	2010

III. 研究成果の刊行物・別刷

代表論文の1報のみ添付する。

TISSUE ENGINEERING: Part C  
Volume 00, Number 00, 2009  
© Mary Ann Liebert, Inc.  
DOI: 10.1089/ten.tec.2009.0608

**Methods Article**

Selective Isolation of Young Cells  
from Human Corneal Endothelium  
by the Sphere-Forming Assay

Tatsuya Mimura, M.D.,<sup>1</sup> Satoru Yamagami, M.D.,<sup>2,3</sup> Seiichi Yokoo, M.D.,<sup>1</sup>  
Tomohiko Usui, M.D.,<sup>1</sup> and Shiro Amano, M.D.<sup>1</sup>

## Selective Isolation of Young Cells from Human Corneal Endothelium by the Sphere-Forming Assay

Tatsuya Mimura, M.D.,<sup>1</sup> Satoru Yamagami, M.D.,<sup>2,3</sup> Seiichi Yokoo, M.D.,<sup>1</sup>  
Tomohiko Usui, M.D.,<sup>1</sup> and Shiro Amano, M.D.<sup>1</sup>

This study aimed to investigate whether a representative adult stem cell/precursor cell isolation method (the sphere-forming assay) could isolate cells with differences of telomere length, telomerase activity, and characteristics reflecting senescence. The sphere-forming assay was performed to obtain precursors from cultured sixth passage (P6) human corneal endothelial cells (CECs). P6 and P7 cultured CECs were used as the controls. Telomere length, telomerase activity, and senescence-associated factors were evaluated in precursors and controls. Precursors obtained from the spheres had longer telomeres and higher telomerase activity than cultured P6 cells. Strong positive staining for senescence-associated  $\beta$ -galactosidase activity was detected in P6 and P7 cultured CECs, whereas little or no staining was detected in the precursors within spheres obtained from P6-cultured CECs or their progeny. The progeny of spheres derived from cultured CECs were small regular cells that grew at a higher density and contained more 5-bromo-2'-deoxyuridine-incorporating cells compared with the parental cultured cells. These findings indicate that the sphere-forming assay enriches precursors with longer telomeres, higher telomerase activity, and younger progeny than the original cells. Thus, the sphere-forming assay may contribute to obtaining the young cells needed for regenerative medicine.

### Introduction

**T**ELOMERES ARE REPETITIVE GENE SEQUENCES that protect the ends of chromosomes. Each time a cell divides, the telomeres become shorter. Telomeres are synthesized and preserved by telomerase, which is a ribonucleoprotein that maintains telomere length by adding G-rich repeats to the ends of eukaryotic chromosomes.<sup>1,2</sup> Telomerase is found at high concentrations in embryonic stem cells, but the amount of telomerase declines with age.<sup>3,4</sup> Telomere length and telomerase activity may affect the ability of adult stem cells to regenerate various tissues.<sup>5</sup>

The sphere-forming assay is a representative technique for the isolation of potential stem cells or precursor cells.<sup>6-13</sup> With this technique, isolated single cells are allowed to proliferate in floating culture and form cell clusters (i.e., sphere colonies) under clonogenic conditions. This technique was initially devised to enrich neural stem cells<sup>1,2</sup> and has since been applied to isolation of multipotential stem cells or precursors from mouse and human skin,<sup>8</sup> mouse inner ear,<sup>9</sup> and human corneal stroma.<sup>13</sup> However, the telomere length and/or telomerase activity in spheres isolated by this assay have not been investigated.

Corneal endothelial cells (CECs) are derived from the neural crest<sup>14,15</sup> and form the corneal endothelial lining as a single layer of hexagonal cells that are considered not to proliferate throughout a person's lifetime.<sup>16</sup> Although human CECs are arrested in the G1 phase of the cell cycle *in vivo*,<sup>17,18</sup> these cells retain the ability to proliferate *in vitro*.<sup>19-22</sup> We have previously isolated spheres from human *ex vivo* CECs and cultured CECs, and have shown that these spheres contain precursor cells.<sup>10,11</sup> Novel techniques that use cultured CECs or precursors obtained by the sphere-forming assay as a cell source may be promising strategies for the development of CEC transplantation in place of conventional corneal transplantation that requires a supply of donor corneas in all cases.<sup>23-30</sup>

Our aim was to investigate whether the sphere-forming assay, that is, multipotential stem cell/precursors isolation method, can be a tool for selective isolation of young cells in cultured cells. In this study, we compared telomere length and telomerase activity among cultured CECs, precursors derived from the cultured CECs, and their progeny. We also evaluated cellular characteristics reflecting senescence when cultured human CECs were grown as a cell sheet for potential use in regenerative medicine.

<sup>1</sup>Department of Ophthalmology, University of Tokyo Graduate School of Medicine, Tokyo, Japan.

<sup>2</sup>Department of Ophthalmology, Tokyo Women's Medical University Medical Center East, Tokyo, Japan.

<sup>3</sup>Corneal Regeneration Research Team Foundation for Biomedical Research and Innovation, Hyogo, Japan.

## Materials and Methods

### Isolation of sphere colonies from cultured human CEC

Human donor corneas were handled according to the tenets of the Declaration of Helsinki of 1975 and its 1983 revision. All of the donor corneas were obtained from Rocky Mountain Lion's Eye Bank. All corneas were considered to be unsuitable for transplantation. Exclusion criteria for donor cornea were low endothelial cell density ( $<2000$  cells/mm<sup>2</sup>); longer than 24 h between time of death and time of preservation; and history of diabetes or glaucoma, sepsis, or ocular infection. Donor ages were 39, 41, 43, and 47 years. All experiments were performed using the same cell line. Primary culture of human CECs was done using a modified version of the protocol described elsewhere.<sup>31</sup> Briefly, CEC was removed from the entire cornea including both the central and peripheral areas. Small explants from the endothelial layer, including Descemet's membrane, were removed with sterile surgical forceps. The explants were placed endothelial cell side down onto four 35-mm tissue culture dishes coated with bovine extracellular matrix, and the dishes were carefully placed in an incubator. This coating dish was prepared by primary bovine CEC culture and CEC removal with trypsin-ethylenediaminetetraacetic acid (EDTA). All the primary cultures and serial passages of CECs were in growth medium consisting of low-glucose Dulbecco's modified Eagle's medium (Invitrogen, Camarillo, CA) supplemented with 15% fetal bovine serum, 2.5 mg/L amphotericin B (Invitrogen), 2.5 mg/L doxycycline, and 2 ng/mL basic fibroblast growth factor (bFGF; Sigma-Aldrich, St. Louis, MO). Cells from the fifth to seventh passages were used for these studies. CECs were incubated in 0.05% trypsin/EDTA (Invitrogen) at 37°C for 5 min, and then were dissociated into single cells by trituration with a fire-polished Pasteur pipette. Isolated CECs had a viability  $>90\%$  as determined by staining with trypan blue (Wako Pure Chemical Industries, Osaka, Japan). The number of cells was determined with a Coulter counter (Beckman-Coulter, Hialeah, FL). The sphere-forming assay was performed for isolation of CEC precursors.<sup>6-13</sup> Basal medium was Dulbecco's modified Eagle's medium/F12 (Invitrogen) supplemented with B27 (Invitrogen), 20 ng/mL epidermal growth factor (Sigma-Aldrich), and 40 ng/mL bFGF. Basal medium containing methylcellulose gel matrix (1.5%; Wako Pure Chemical Industries) was used to prevent the re-aggregation of cells, as described elsewhere.<sup>10,11</sup> Cultured passage 5 (P5) or P6 CECs were cultured at a density of 10 viable cells/ $\mu$ L (40,000 cells per well or 1415 cells/cm<sup>2</sup>) in nontissue 60-mm culture dishes (BD Labware, Bedford, MA) to obtain spheres. To distinguish growing spheres from dying cell clusters, only clusters with a diameter of more than 50  $\mu$ m were used. For passaging, primary spheres (day 7) were treated with 0.05% trypsin/0.02% EDTA and dissociated into single cells that were added to 24-well culture plates at a density of 10 cell/ $\mu$ L. To obtain their progenies, individual free-floating primary spheres (day 7) were collected and subcultured separately by plating in 24-well culture dishes.

P6 CECs obtained from cultured P5 CECs or precursors obtained from the same P5 CECs were used to construct the cell sheets. Late-passage CECs (P6 and P7) or precursors derived from P6 CECs were used for *in vitro* investigation of senescence-associated  $\beta$ -galactosidase (SA- $\beta$ -Gal) activity, the

length of telomere repeats, and telomerase activity to examine differences between cultured CECs and precursors, because these studies required an extremely large number of cells.

### Evaluation of SA- $\beta$ -Gal activity

Detection of SA- $\beta$ -Gal activity was performed with a commercial Senescence Detection Kit (BioVision Research Products, Mountain View, CA) according to the manufacturer's instructions. We used cultured cells or spheres from four donor corneas (39, 41, 43, and 47 years of age). Late-passage cells (P6 and P7) were prepared for the measurement of SA- $\beta$ -Gal activity and telomere length. Confluent day 7 P6 or P7 CECs, day 7 spheres derived from P6 CECs, or day 7 progeny derived from spheres were stained with SA- $\beta$ -Gal, as described elsewhere.<sup>32</sup> Briefly, confluent cells in 24-well plates or spheres were washed with Ca<sup>2+</sup>- and Mg<sup>2+</sup>-free Dulbecco's phosphate-buffered saline (PBS; Sigma-Aldrich), fixed for 15 min at room temperature, and then incubated overnight at 37°C in a staining solution that contained 5-bromo-4-chloro-3-indoyl-galactopyranoside at pH 6.0 according to the manufacturer's protocol. On the next day, the cells were washed with PBS for 15 min. A blue color indicated the presence of SA- $\beta$ -Gal activity. Staining was observed at a 20-fold magnification, and bright-field photomicrographs of the central area of each dish were obtained with a microscope (BX50; Olympus, Tokyo, Japan). Images were evaluated on a computer (Photoshop version 6.0; Adobe Systems, San Jose, CA). The intensity of SA- $\beta$ -Gal activity was graded in each cell as follows: 0, no staining; 1, focal weak staining; 2, multifocal moderate staining; and 3, multifocal intense staining (see Fig. 2E). Graded cells were counted with Image-J software (<http://rsb.info.nih.gov/ij/>) developed by Wayne Rasband and provided in the public domain by National Institutes of Health, Bethesda, MD). Individual cells were identified for counting through observation of their borders by bright-field microscopy. The number of cells that showed staining for SA- $\beta$ -Gal and the grade of SA- $\beta$ -Gal activity in four photographs from four dishes (800 $\times$ 600  $\mu$ m) were averaged. Cells with unclear images were eliminated from assessment. The average total number of cells counted was 714.3 cells. The percentage of cells stained for SA- $\beta$ -Gal was calculated with the following formula:  $100 \times (\text{number of cells stained by SA-}\beta\text{-Gal} / \text{total number of cells})$ .

As for the preparation of spheres, the collected free-floating spheres were placed in 24-well plates, stained with SA- $\beta$ -Gal under the same conditions as used for the cells on the tissue culture dishes, and observed under the microscope. The total number of spheres counted was 45. SA- $\beta$ -Gal-stained cultures were evaluated in a masked fashion by two observers and there was no difference between the results of the two observers.

### Southern blot analyses of telomere repeat length

The cells from the cornea of a 41-year-old donor were used in this study. P6 or P7 CECs cultured for 7 days (almost confluent), day 7 spheres derived from P6 CECs, and day 7 progenies from P6 CECs derived from spheres (almost confluent) were stored at  $-70^\circ\text{C}$  until DNA was isolated. DNA was isolated with a Gentra DNA Purification Kit (Gentra Systems, Minneapolis, MN) according to the manufacturer's protocol. Briefly, cells were minced in TNE (10 mM, Tris



hydrochloride [pH 7.5], 100 mM NaCl, and 10 mM EDTA), sodium dodecyl sulfate (SDS, 0.5%) and proteinase K (100 µg/mL) were added, and DNA was incubated at 55°C for at least 1 h. Then, DNA was isolated by phenol-chloroform extraction and precipitation with isopropanol. Incubation with proteinase K and extraction were repeated once, and DNA thus obtained was dissolved in TE (10 mM Tris hydrochloride [pH 7.5] and 0.1 mM EDTA) at 200 to 500 µg/mL and stored at 4°C. Extracted DNA (10 µg) was completely digested with *HinfI* (Takara Shuzo, Otsu, Japan) to measure the length of the telomere repeats. Digested DNA was precipitated in ethanol, resuspended in TE (pH 8.0), and subjected to spectrophotometry to assess purity and quantity. Digested DNA (10 µg/lane) was loaded onto 0.8% agarose gels (SeaKem GTG; Cambrex Bio Science Rockland Inc., Rockland, ME) for electrophoresis. DNA was denatured by soaking the gels in 0.5 M NaOH with 1.5 M NaCl twice for 30 min each, and then in 0.5 M Tris hydrochloride (pH 7.5) with 3 M NaCl twice for 30 min. Then, DNA was transferred to a nylon membrane (Hybond N; GE Healthcare Bio-Sciences, Piscataway, NJ). Probes were labeled with [ $\gamma$ - $^{32}$ P]-ATP (GE Healthcare Bio-Sciences) by using a 5' end-labeling kit (Megalabel; Takara Bio, Shiga, Japan). The DNA target was prehybridized overnight at 65°C with denatured salmon sperm DNA (Wako Pure Chemical Industries), and then was hybridized overnight at 50°C with a 5'-end [ $\gamma$ - $^{32}$ P]-labeled repeat (TTAGGG)<sub>4</sub> (Greiner, Frickenhausen, Germany) in 10× modified Denhart's solution with 1 M NaCl, 50 mM Tris-HCl (pH 7.4), 10 mM EDTA, 0.1% SDS, and 50 µg/mL denatured salmon sperm DNA. Membranes were washed twice with 2× standard saline citrate (pH 7.0) containing 2% SDS at 50°C for 30 min, as well as once with 0.1× standard saline citrate containing 0.1% SDS at 50°C for 30 min. Then, autoradiography was done with a BAS-5000 (Fujifilm, Tokyo, Japan). The signal intensity was measured using ImageGauge software (Fujifilm Medical System, Stamford, CT), and the signal peaks were used to estimate the lengths of telomere repeats. Circularized  $\lambda$ -*Hind* III DNA fragments were used as molecular markers (from top to bottom: 23.1, 9.4, 6.6, 4.3, 2.3, and 2.0 kb). Southern blot analyses of telomere repeat length require a large number of cells (i.e., 1,000,000 cells) and we used spheres from 20 non-tissue 60-mm culture dishes with one experiment. The cultured cells from donors other than a 41-year-old donor could not be used for this experiment because of the insufficient number of cells.

#### Telomerase activity

We performed four experiments per each cell line from four donor corneas (39, 41, 43, and 47 years old). Our preliminary observations showed little or no telomerase activity in P6 confluent CECs. Therefore, we used subconfluent P6 or P7 CECs cultured for 6 days, day 6 spheres derived from P6 CECs, and subconfluent day 6 progeny derived from the spheres to compare the telomerase activity of proliferating spheres with that of cultured cells. All samples were stored at -70°C. For analysis of telomerase activity, the Telo TAGGG Telomerase PCR Elisaplus kit (Roche Diagnostics, Mannheim, Germany) was employed according to the manufacturer's instructions. This assay is based on the internal activity of telomerase, with the product being amplified by polymerase chain reaction (PCR) and detected with an

enzyme-linked immunosorbent assay that was an extension of the telomeric repeat amplification protocol originally described by Kim *et al.*<sup>33</sup> Cell lysates obtained from  $2 \times 10^5$  cells were analyzed by PCR to detect telomerase activity. This was a two-step process in which telomerase-mediated elongation products were subsequently amplified by PCR to allow highly sensitive detection of telomerase activity. A 216 bp homologous standard (internal standard) provided with the kit allowed clear detection of Taq DNA polymerase inhibitors. Each sample (5 µL) was inactivated by incubation at 95°C for 10 min before performing the telomeric repeat amplification protocol assay to inactivate telomerase protein and produce negative controls. PCR was done in a thermal cycler (I-Cycler; Bio-Rad Laboratories, Hercules, CA) with primer elongation for 1 cycle at 25°C for 30 min, telomerase inactivation for 1 cycle at 94°C for 5 min, amplification (denaturation) for 1 to 30 cycles at 94°C for 30 s, annealing at 50°C for 30 s, polymerization at 72°C for 90 s, and final extension at 72°C for 10 min. An aliquot of the PCR products was denatured and hybridized to a digoxigenin-labeled, telomeric-repeat-specific detection probe. This hybrid was then immobilized to a streptavidin-coated microtiter plate by the biotin-labeled primer. Finally, the digoxigenin label was detected with anti-digoxigenin peroxidase. The probe was observed by peroxidase metabolizing tetramethyl benzidine to form a colored reaction product, and the intensity of the color was measured at 450 nm with a microtiter plate reader (ARVO™ MX 1420 multilabel counter; Perkin Elmer Japan, Yokohama, Japan). Four different experiments were analyzed for quantification. Mean values calculated from the four experiments were averaged in each cell line.

#### Human amniotic membranes

This study was approved by the Human Studies Review Board of the University of Tokyo Graduate School of Medicine and was performed in accordance with the 1975 Declaration of Helsinki and its 1983 revision. After informed consent was obtained from each subject, human placentas were harvested under sterile conditions at elective cesarean section. The amniotic membrane was dissected from the chorion with forceps and washed several times with sterile saline to remove any adherent blood clots. Under sterile conditions, the amniotic membrane was then rinsed three times in PBS containing 0.1 mg/mL streptomycin (Sigma-Aldrich) and 0.25 µg/mL amphotericin B (Sigma-Aldrich), and was cut into pieces measuring approximately 3.0×3.0 cm. These tissue pieces were frozen and stored at -80°C in a cell bank (Wako Pure Chemical Industries). Amniotic tissues were thawed by warming to room temperatures for 10 min, rinsed three times in saline, and incubated in PBS with 0.02% EDTA at 37°C for 180 min to loosen the amniotic epithelial cells. Then, the epithelial cells and residual chorion were removed by gentle scraping with a cell scraper (Becton Dickinson, Lincoln Park, NJ), and the membrane pieces were washed three times with PBS.

#### Migration and proliferation of CE spheres on human Descemet's membrane *ex vivo*

Day 7 spheres derived from P6 CECs were labeled with a fluorescent cell tracker (CM-DiI; C-7000; Molecular Probes, Eugene, OR). DiI-labeled spheres were seeded onto the

denuded Descemet's membrane in culture, after which the corneas were placed in 24-well plates. The plated corneas were maintained in culture medium for 7 days. Fluorescence of spheres that migrated was viewed under a fluorescence microscope, and the area occupied with cells that had migrated from the spheres was measured by the National Institutes of Health Image program ( $n = 10$ ).

#### Construction of a human CEC sheet using precursors

Pieces of acellular amniotic membrane ( $2.0 \times 2.0$  cm) were spread, basement membrane side up, on the bottom of 24-well culture plates. Primary spheres (day 7) derived from cultured P5 CECs were treated with 0.5% EDTA and dissociated into single cells, which were plated at a density of 530 viable cells/ $\mu\text{L}$  ( $5.3 \times 10^5$  cells/well or 3000 cells/ $\text{mm}^2$ ) on the denuded amniotic membranes and maintained in low glucose Dulbecco's modified Eagle's medium (Invitrogen) supplemented with 15% fetal bovine serum and 2 ng/mL bFGF for another 2 days. As a control, cells from P5 CECs were cultured under the same conditions.

After growth of the cell sheet, cell morphology and density were evaluated under an inverted phase-contrast microscope. The number of cells in a  $0.1 \times 0.1$  mm square was counted at four different sites on each of four sheets constructed from CECs and CEC precursors. Then, the cell sheets were bisected for immunohistochemical analysis.

#### Histological examination

Cell sheets were fixed in PBS with 4% paraformaldehyde (Wako Pure Chemical Industries) for 10 min. After being washed in PBS, the cell sheets were incubated for 30 min with 3% bovine serum albumin (BSA; Sigma-Aldrich) in PBS containing 0.3% Triton X-100 (Rohm & Haas, Philadelphia, PA) (BSA/PBST) to block nonspecific binding. Then, the sheets were incubated for 2 h at room temperature with the following specific primary antibodies diluted in BSA/PBST: mouse anti-cytokeratin 3 monoclonal antibody (mAb, AE-5; Progen Biotechnik, Heidelberg, Germany), rabbit anti-ZO-1 Ab (1:400; Invitrogen), mouse anti-nestin mAb (1:400; Becton Dickinson), or mouse anti-bromodeoxyuridine (BrdU)/fluorescence mAb (1:100; Roche Diagnostics, Basel, Switzerland). As for staining of ZO-1, nuclei were counterstained with Hoechst 33342 (1:2000; Molecular Probes). Mouse immunoglobulin (IgG; 1:1000; Sigma-Aldrich) was used as the

control in place of the primary antibody. After being washed in PBS, the cell sheets were reacted for 1 h at room temperature with fluorescence-labeled goat anti-mouse IgG (Alexa Fluor 488, 1:2000; Molecular Probes) and fluorescence-labeled goat anti-rabbit IgG (Alexa Fluor 594, 1:400; Molecular Probes) as the secondary antibody. Fluorescence was observed under a fluorescence microscope (model BH2-RFL-T3 and BX50; Olympus).

#### Statistics

One-way analysis of variance and Scheffe's multiple comparison test were used to compare mean values. The level of significance was set at  $p < 0.05$ . All analyses were performed with the Stat View statistical software package (Version 5; Abacus Concepts, Berkeley, CA).

#### Results

##### Sphere formation from P6-cultured human CECs

P6-cultured human CECs (Fig. 1A) were disaggregated into single cells that were cultured under floating conditions for 7 days. As a result, spheres developed and grew larger, while nonproliferating cells were eliminated. Representative images of growing spheres are shown in Figure 1. Only single cells were observed in culture medium containing methylcellulose gel matrix that prevented re-aggregation (Fig. 1B). Spheres developed from the single cell suspension on day 3 (Fig. 1C) and grew larger by day 7 (Fig. 1D). Many cells migrated from the sphere colonies (Fig. 1D), and the progenies from sphere colonies could be passaged twice. The number of sphere colonies obtained from the P6 CECs after 7 days of culture was  $42.3 \pm 7.9$  per 10,000 cells (mean  $\pm$  standard deviation). When the primary sphere colonies from P5 CECs were dissociated into single cells and were cultured in the presence of methylcellulose gel matrix, secondary and tertiary sphere colonies were generated. To estimate the number of spheres needed to cover the inner surface of the cornea (Descemet's membrane), DiI-labeled spheres were prepared and seeded onto the denuded Descemet's membrane in culture. The mean area covered per DiI-labeled sphere was  $1.2 \pm 0.2$   $\text{mm}^2$  on day 7. Therefore, the number of spheres needed per cornea was calculated to be 75. Approximately 150 spheres may be enough to use for clinical cases to allow for loss of spheres that failed to adhere.<sup>11</sup>

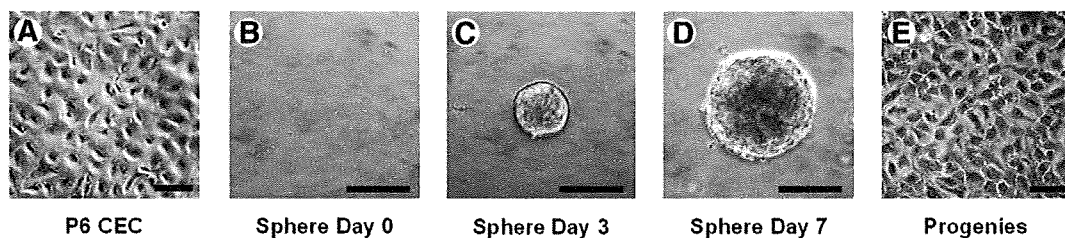


FIG. 1. Representative sphere formation from passage 6 (P6)-cultured human corneal endothelial cells (CECs). P6-cultured CECs are derived from a 43-year-old donor (A). Single cells were grown under serum-free floating culture conditions for 7 days. Dissociated single cells are observed in medium containing methylcellulose gel matrix (B). A sphere colony has grown from a single cell on day 3 (C) and has become large on day 7 (D). Adherent progenies migrate from the sphere colonies (E). Scale bars = 100  $\mu\text{m}$ .

*SA-β-Gal activity of cultured human CECs or CEC precursors*

Cells were stained for SA-β-Gal to determine the proportion of senescent cells in each population. Positive staining for SA-β-Gal activity was detected in P6-cultured human CECs (Fig. 2A) and prominent-positive staining was observed in P7-cultured human CECs (Fig. 2B), whereas little staining was detected in the precursors within spheres derived from P6-cultured CECs (Fig. 2C, D) or their progeny (Fig. 2E). SA-β-Gal staining was graded to measure the relative staining intensity. Micrographs in Figure 2F illustrate the different grades of SA-β-Gal staining observed in the cultured CECs. The graph in Figure 2G shows that the percentage of CECs

positive for SA-β-Gal was higher in P7 than P6 cultures (96.8% ± 11.4% vs. 68.5 ± 4.2%). No SA-β-Gal staining was observed in the precursors within spheres. Among the progeny derived from spheres, the percentage of cells showing SA-β-Gal staining was 80.9% ± 3.4% at an intensity of 0, 14.7% ± 4.2% at 1, 3.3% ± 1.2% at 2, and 0.0% ± 0.0% at 3. SA-β-Gal staining in the progeny was less than that in P6- and P7-cultured CECs.

*Length of telomere repeats*

The average telomere length was calculated based on the results of Southern blotting. P7-cultured human CECs had shorter telomeres (9.5 kb) than P6 human CECs (10.4 kb),

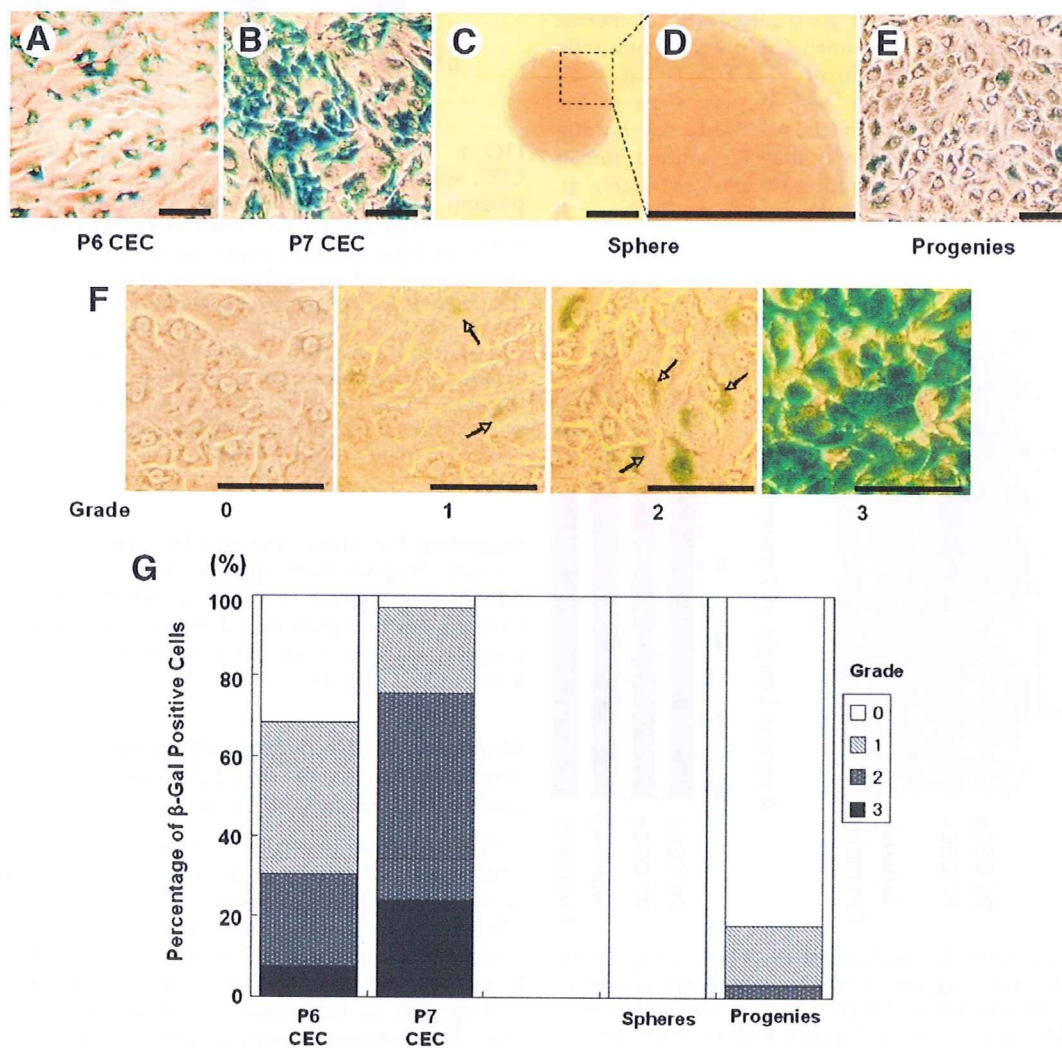


**FIG. 2.** Histochemical analysis (A–E) and scoring (F, G) of senescence-associated β-galactosidase (SA-β-Gal) activity in P6- and P7-cultured human CECs, spheres derived from P6-cultured CECs, and the progeny of the spheres. Cells are derived from four donor corneas and photographs show representative cell images from cornea of a 47-year-old donor. Cells were cultured for 7 days. There is a low level of positive SA-β-Gal staining in P6 CECs (A), and increased staining in P7 CECs (B). There is no SA-β-Gal staining of the precursors within a sphere (C, D) and little positive SA-β-Gal staining of the progeny derived from a sphere (E). SA-β-Gal intensity was graded as 0 (no staining), 1 (focal weak staining), 2 (multifocal moderate staining), or 3 (multifocal intense staining) as shown in (F). (G) Average percentage of SA-β-Gal-positive cells in each grade. Experiments were repeated four times with substantially similar results and the data were averaged. Scale bars: (A–F) 100 μm.

confirming that passaging of cells shortens telomere repeat length *in vitro* (Fig. 3). The average telomere length of precursor cells within spheres (11.4 kb) and their progeny (10.6 kb) was longer than that of P7-cultured human CECs (9.5 kb).

#### Telomerase activity

Absorbance by the internal standards at 450 nm ranged between 0.691 and 0.717, and negative controls ranged between 0.052 and 0.063. No significant differences were detected with respect to the mean levels for internal standards and negative controls among the four groups (Fig. 4). Little or no telomerase activity was detected in P6 and P7 confluent CECs (data not shown). One-way analysis of variance showed significant differences in the telomerase activity among four groups ( $F = 10.685$ ,  $p = 0.00105$ ). The telomerase activity of subconfluent P6 human CECs was significantly higher than that of subconfluent P7 CECs ( $p = 0.01725$ , Scheffe's multiple comparison test, Fig. 4). Cells in the spheres derived from P6 human CECs showed a significantly higher level of telomerase activity than P6-cultured human CECs ( $p = 0.02665$ , Scheffe's multiple comparison test, Fig. 4),

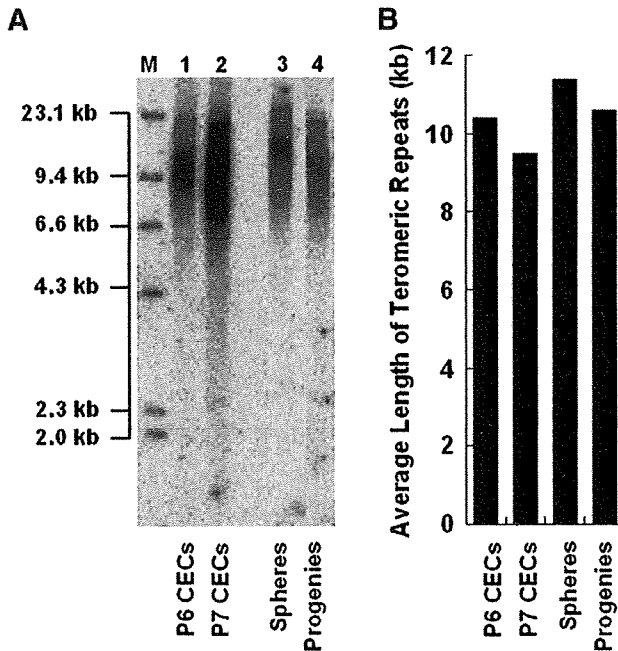


FIG. 3. Southern blot analysis of the length of telomeric repeats (A) and diagram showing the average length of telomeres (B) in each cell type. Cells are derived from a 41-year-old donor. DNA was digested with the restriction enzyme *HinfI* and hybridized with the  $^{32}\text{P}$ -labeled (TTAGGG)<sub>4</sub> probe. The average length of telomeres in the precursors from spheres (11.4 kb) and their progeny (10.6 kb) was longer than that of P7-cultured human CECs (9.5 kb). Markers were  $\lambda$  DNA/*Hind III* fragments (from top to bottom: 23.1, 9.4, 6.6, 4.3, 2.3, and 2.0 kb). Lane M, molecular marker; lane 1, P6 CEC; lane 2, P7 CEC; lane 3, precursors from a sphere derived from P6 CEC; lane 4, progeny derived from a sphere. Average telomere length is shown as bars (B).

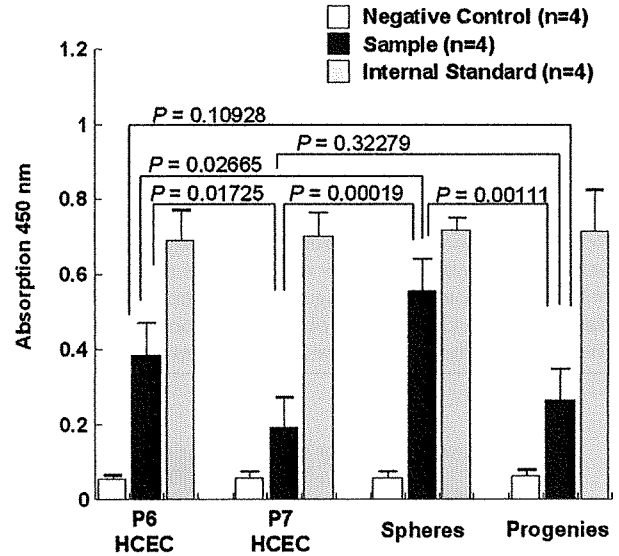
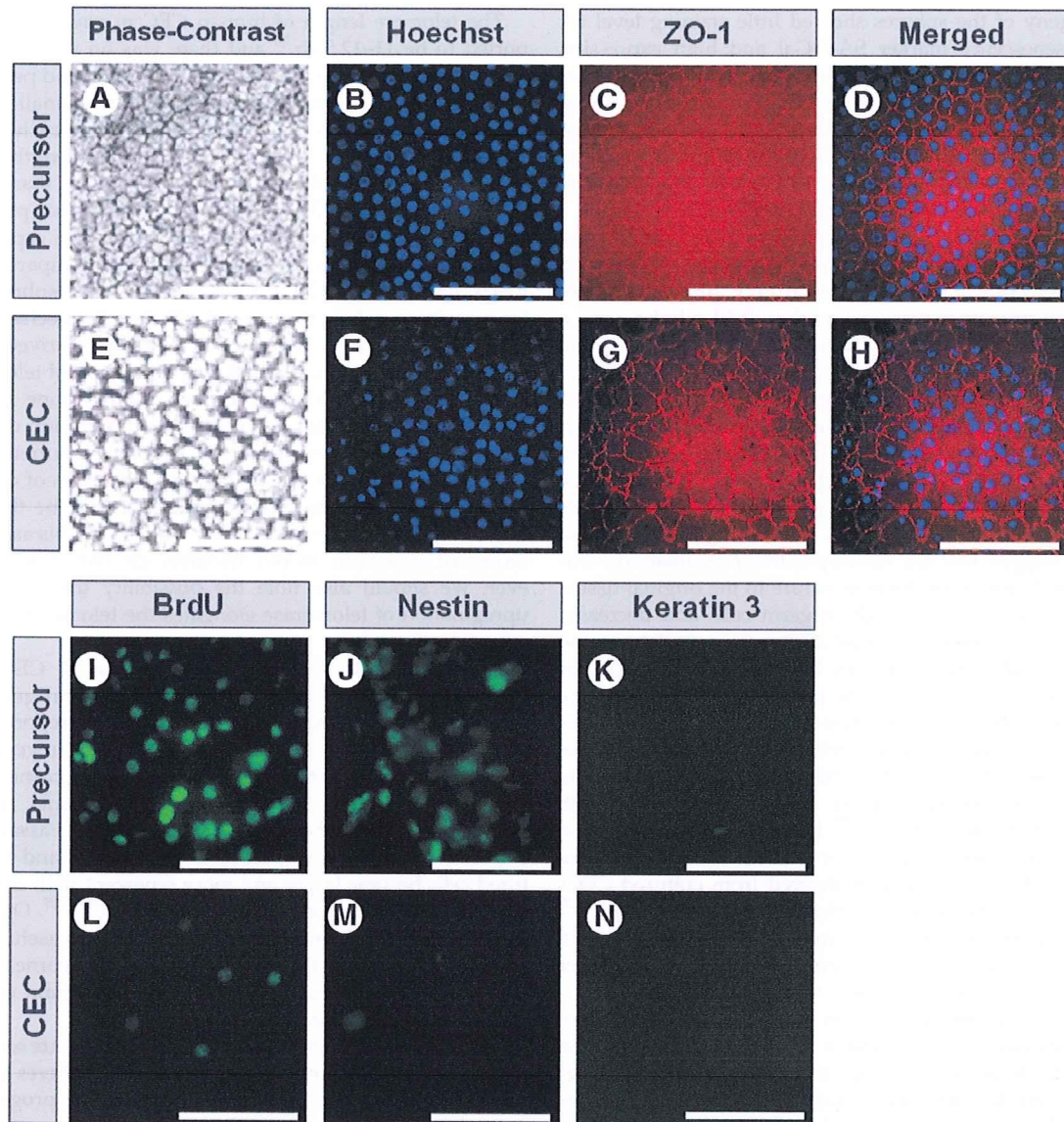


FIG. 4. Telomerase activity in P6- and P7-cultured human CEC, spheres derived from P6-cultured human CEC, and progeny of the spheres. Cells were cultured for 6 days and then analyzed using a Telo TAGGG Telomerase PCR ELISA PLUS kit. Heat-treated samples were employed as the negative control, and internal standards provided in the kit were the positive control. Error bars show the standard deviation ( $n = 4$  each). Telomerase activity is significantly lower in P7-cultured CECs than in P6-cultured CECs. The cells of spheres derived from P6 CECs show significantly higher telomerase activity than P6-cultured CECs. One-way analysis of variance and Scheffe's multiple comparison tests were used to compare mean values.

suggesting that these cells had the capacity to proliferate actively. Progeny from spheres showed lower telomerase activity than spheres ( $p = 0.00112$ , Scheffe's multiple comparison), but no significant difference was detected between progeny and P6 human CECs or between progeny and P7 human CECs (Fig. 4).

#### Morphology of cells in human CEC sheets constituted from human P5 CEC-derived precursors or P6-cultured CECs

We used a thin transparent denuded amniotic membrane, which consisted entirely of amniotic stroma and was devoid of epithelial cells and chorion. We could observe clearly CECs through the transparent amniotic membrane using an inverted phase-contrast microscope. The cells obtained from P5 CEC-derived spheres showed a typical CEC morphology as they grew on the amniotic membrane 48 h after seeding (Fig. 5). Histological examination revealed a hexagonal monolayer of CEC precursors anchored to the membrane. The cell density was 35.5% higher in the CEC precursor sheets created from P5 CEC-derived spheres ( $n = 4$ ) than in P6-cultured CEC sheets ( $n = 4$ ), and there was a significant difference between the two groups ( $p = 0.00051$ , unpaired *t*-test). Figure 5C and G shows expression of the tight junction protein ZO-1 by CECs. Cells in the precursor sheets cultured on amniotic membranes had a CEC-like regular



**FIG. 5.** Construction of cell sheets using human CEC precursors (A–D, I–K) or cultured human CECs (E–H, L–N). Cells are derived from a 39-year-old donor. Precursor cells from P5-cultured CEC-derived spheres dissociated with ethylenediaminetetraacetic acid or P6-cultured human CECs were seeded on amniotic membrane pieces and maintained in serum-free culture medium. After 48 h, the adherent and proliferating precursor cells achieved a higher density on the amniotic membrane compared with P6-cultured CECs (A, E). P5 CEC-derived precursor cells (B–D) have a more regular hexagonal shape than P6 cultured CECs (F–H), as shown by staining for ZO-1 (D, H). Nuclei counterstained with Hoechst 33342 (B, F). P5 CEC-derived precursors demonstrate considerably more positive staining for bromodeoxyuridine (BrdU) (I, L) and nestin (J, M) compared with P6-cultured CEC. No staining for corneal-epithelium-specific cytokeratin 3 is detected in either type of cell (K, N). Scale bars represent 100  $\mu$ m.

hexagonal shape (Fig. 5C), unlike the variable shape and size of cells in the sheets derived from cultured CECs (Fig. 5G).

A larger number of BrdU- and nestin-positive cells were detected in P5 CEC-derived precursor sheets compared with P6-cultured CEC sheets (Fig. 5I, J, L, M). Cytokeratin 3-positive cells were not observed in either type of cell sheet, indicating no contamination by corneal epithelial cells (Fig. 5K, N).

## Discussion

Cellular senescence is characterized by enlargement of cells, inability to regenerate, and an increase of SA- $\beta$ -gal activity, and is induced by critical telomere shortening.<sup>34</sup> Our findings clearly demonstrated that cells isolated from cultured CECs by the sphere-forming assay had longer telomeres and higher telomerase activity than the original cells.

The progeny of the spheres showed little staining level for the cell senescence marker SA- $\beta$ -Gal and high expression of the immature cell marker nestin. They also had a regular morphology and grew at a higher density with greater BrdU incorporation than passaged cells derived from the same parental cells. These findings indicate that the sphere-forming assay is an easy and useful method of isolating young (precursor) cells from various other cells.

The corneal endothelium is derived from the neural crest and our previous study demonstrated that spheres derived from donor corneal CEC express an immature cell marker (nestin), an immature neuronal marker ( $\beta$ -III tubulin), and a mature glial cell marker, whereas their progenies express  $\beta$ -III tubulin and nestin.<sup>10</sup> In contrast, the progenies of precursors derived from cultured human CECs show decreased expression of immature cell markers (nestin).<sup>11</sup> Additionally, nestin is localized in the precursor cells in the posterior limbus of human cornea.<sup>35</sup> A larger number of nestin-positive cells were detected in P5 CEC-derived precursor sheets compared with P6-cultured CEC sheets (Fig. 5J, M). These findings suggest that the nestin-positive precursors on amniotic membrane were closer in nature to the original tissue.

Telomerase activity is high in germ cells and decreases in the sperm and ova.<sup>4</sup> In almost all somatic cells, telomerase activity is undetectable or very low. In human CECs, the telomerase was localized in the peripheral CECs,<sup>35</sup> but the central CECs show no telomerase activity.<sup>36</sup> Adult stem cells also show undetectable or low telomerase activity regardless of their proliferative capacity, whereas committed precursors with high proliferative activity have comparatively high levels of telomerase activity.<sup>4,37</sup> However, their telomerase activity is still not adequate for maintenance of telomere length.<sup>4</sup> In this study, spheres derived from cultured CECs (i.e., CEC precursors with limited self-renewal capacity)<sup>29</sup> showed higher telomerase activity that was consistent with the characteristics of lineage-committed precursors rather than adult stem cells with lower telomerase activity.

The level of telomerase activity is associated with the proliferative capacity of cells<sup>38</sup> and *in vitro* mitogenic stimulation upregulates telomerase activity in human lymphocytes despite the very low telomerase activity of unstimulated lymphocytes.<sup>39</sup> In our present study, little or no telomerase activity was detected in confluent cultured cells (data not shown). Therefore, we used subconfluent cultured cells as the control for comparison with the telomerase activity of proliferating spheres in floating culture. The moderate telomerase activity of cultured CECs and high telomerase activity of proliferating spheres are consistent with previous findings,<sup>4,38,39</sup> so our experimental design seemed to be appropriate for evaluation of telomerase activity in these cells. The telomerase activity of the subconfluent progeny was intermediate between that of the P6 and P7 CECs and much lower than the spheres from which they were derived. These results suggest that the progeny possesses a higher-proliferative potential than the passaged P7 CECs. Additionally, progeny from sphere colonies could be passaged twice and showed almost same doubling times. Secondary and tertiary sphere colonies were generated from the primary sphere colonies from P5 CECs, but quaternary colonies were not generated. These results indicate that the capacity for self-renewal of sphere colonies derived from cultured CECs is limited.

The telomere length of human CEC *in vivo* has been reported to be 11–12.5 kb,<sup>20</sup> and there was no significant difference in telomere length between the central and peripheral areas of human donor corneas.<sup>40</sup> Normally, a small amount of telomeric DNA (~50–100 bp) is lost with each human somatic cell division.<sup>41</sup> The average telomere length of precursor cells within spheres (11.4 kb) was longer than that of P7-cultured human CECs (9.5 kb), suggesting that precursor cells within sphere possess stronger replicative capacity of approximately 19–38 divisions in culture compared with P7-cultured human CECs. Cells isolated from spheres had longer telomeres than the original cells, but the mechanism by which telomeres were elongated in the sphere-derived cells is unknown. It was reported that overexpression of telomerase leads to elongation of telomeres in human bone marrow stromal cells,<sup>42</sup> whereas telomerase overexpression does not prevent proliferation-associated telomere shortening in human hematopoietic cells.<sup>43</sup> Because only 0.5% of cultured human CECs are sphere-forming cells, it may be that cells with long telomeres are selectively isolated by this assay and senescent cells with shorter telomere are eliminated. However, we should also note the possibility that temporary upregulation of telomerase elongates the telomeres to some extent during culture.

With respect to the clinical application of CEC sheet transplantation in place of full thickness corneal grafts, the feasibility of harvesting cultured CECs has been reported.<sup>23–30</sup> Cultured CECs are an attractive source for regenerative medicine because there are not enough donor corneas anywhere in the world, while cultured CECs could create a number of corneal sheets for transplantation. Passaging of cultured CECs, however, leads to senescence, and the cultured cells become larger and more senescent with older donor age and increasing passage number.<sup>31,44,45</sup> Our data suggest that the sphere-forming assay could be a useful tool to maximize the number of CECs from a donor cornea and it may even become a standard technique to obtain cells for regenerative medicine.

In summary, the sphere-forming assay can isolate cells with longer telomeres from cultured CECs. The spheres contain precursors with a high telomerase activity. The progeny derived from spheres show little staining for the senescence marker SA- $\beta$ -Gal, have a regular morphology, and grow at a higher density compared with passaged CECs from the same source. These findings indicate that the sphere-forming assay enriches precursors with longer telomeres, higher telomerase activity, and younger progeny than the original cells, and it may contribute to obtaining the young cells needed for regenerative medicine.

#### Acknowledgments

This work was supported by a Grant-in-Aid for Scientific Research from the Ministry of Education, Culture, Sports, Science and Technology of Japan.

#### Disclosure Statement

No competing financial interests exist. The authors have no commercial or proprietary interest in the product or company described in the current article. Satoru Yamagami

had full access to all the data in the study and takes responsibility for the integrity of the data and the accuracy of the data analysis.

## References

- Lin, K.W., and Yan, J. The telomere length dynamic and methods of its assessment. *J Cell Mol Med* **9**, 977, 2005.
- Shin, J.S., Hong, A., Solomon, M.J., and Lee, C.S. The role of telomeres and telomerase in the pathology of human cancer and aging. *Pathology* **38**, 103, 2006.
- Sethe, S., Scutt, A., and Stolzing, A. Aging of mesenchymal stem cells. *Ageing Res Rev* **5**, 91, 2006.
- Hiyama, E., and Hiyama, K. Telomere and telomerase in stem cells. *Br J Cancer* **96**, 1020, 2007.
- Sharpless, N.E., and DePinho, R.A. Telomeres, stem cells, senescence, and cancer. *J Clin Invest* **113**, 160, 2004.
- Reynolds, B.A., and Weiss, S. Generation of neurons and astrocytes from isolated cells of the adult mammalian central nervous system. *Science* **255**, 1707, 2000.
- Gage, F.H. Mammalian neural stem cells. *Science* **287**, 1433, 2000.
- Toma, J.G., Akhavan, M., Fernandes, K.J., Barnabé-Heider, F., Sadikot, A., Kaplan, D.R., and Miller, F.D. Isolation of multipotent adult stem cells from the dermis of mammalian skin. *Nat Cell Biol* **3**, 778, 2001.
- Li, H., Liu, H., and Heller, S. Pluripotent stem cells from the adult mouse inner ear. *Nat Med* **9**, 1293, 2003.
- Yokoo, S., Yamagami, S., Yanagi, Y., Uchida, S., Mimura, T., Usui, T., and Amano, S. Human corneal endothelial cell precursors isolated by sphere-forming assay. *Invest Ophthalmol Vis Sci* **46**, 1626, 2005.
- Mimura, T., Yokoo, S., Araie, M., Amano, S., and Yamagami, S. Treatment of rabbit bullous keratopathy with precursors derived from cultured human corneal endothelium. *Invest Ophthalmol Vis Sci* **46**, 3637, 2005.
- Uchida, S., Yokoo, S., Yanagi, Y., Usui, T., Yokota, C., Mimura, T., Araie, M., Yamagami, S., and Amano, S. Sphere formation and expression of neural proteins by human corneal stromal cells *in vitro*. *Invest Ophthalmol Vis Sci* **46**, 1620, 2005.
- Yoshida, S., Shimmura, S., Nagoshi, N., Fukuda, K., Matsuzaki, Y., Okano, H., and Tsubota, K. Isolation of multipotent neural crest-derived stem cells from the adult mouse cornea. *Stem Cells* **24**, 2714, 2006.
- Johnston, M.C., Noden, D.M., Hazelton, R.D., Coulombre, J.L., and Coulombre, A.J. Origins of avian ocular and periocular tissues. *Exp Eye Res* **29**, 27, 1979.
- Bahn, C.F., Falls, H.F., Varley, G.A., Meyer, R.F., Edelhauser, H.F., and Bourne, W.M. Classification of corneal endothelial disorders based on neural crest origin. *Ophthalmology* **91**, 558, 1984.
- Murphy, C., Alvarado, J., Juster, R., and Maglio, M. Prenatal and postnatal cellularity of the human corneal endothelium. A quantitative histologic study. *Invest Ophthalmol Vis Sci* **25**, 312, 1984.
- Joyce, N.C., Mekler, B., Joyce, S.J., and Zieske, J.D. Cell cycle protein expression and proliferative status in human corneal cells. *Invest Ophthalmol Vis Sci* **37**, 645, 1996.
- Joyce, N.C., Navon, S.E., Roy, S., and Zieske, J.D. Expression of cell cycle-associated proteins in human and rabbit corneal endothelium *in situ*. *Invest Ophthalmol Vis Sci* **37**, 1566, 1996.
- Wilson, S.E., Weng, J., Blair, S., He, Y.G., and Lloyd, S. Expression of E6/E7 or SV40 large T antigen-coding oncogenes in human corneal endothelial cells indicates regulated high-proliferative capacity. *Invest Ophthalmol Vis Sci* **36**, 32, 1995.
- Egan, C.A., Savre-Train, I., Shay, J.W., Wilson, S.E., and Bourne, W.M. Analysis of telomere lengths in human corneal endothelial cells from donors of different ages. *Invest Ophthalmol Vis Sci* **39**, 648, 1998.
- Senoo, T., and Joyce, N.C. Cell cycle kinetics in corneal endothelium from old and young donors. *Invest Ophthalmol Vis Sci* **41**, 660, 2000.
- Joyce, N.C. Proliferative capacity of the corneal endothelium. *Prog Retin Eye Res* **22**, 359, 2003.
- Aboalchamat, B., Engelmann, K., Böhnke, M., Eggli, P., and Bednarz, J. Morphological and functional analysis of immortalized human corneal endothelial cells after transplantation. *Exp Eye Res* **69**, 547, 1999.
- Engelmann, K., and Friedl, P. Optimization of culture conditions for human corneal endothelial cells *in vitro*. *Cell Dev Biol* **25**, 1065, 1989.
- Engelmann, K., Drexler, D., and Böhnke, M. Transplantation of adult human or porcine corneal endothelial cells onto human recipients *in vitro*. Part I: cell culturing and transplantation procedure. *Cornea* **18**, 199, 1999.
- Böhnke, M., Eggli, P., and Engelmann, K. Transplantation of cultured adult human or porcine corneal endothelial cells onto human recipients *in vitro*. Part II: evaluation in the scanning electron microscope. *Cornea* **18**, 207, 1999.
- Chen, K.H., Azar, D., and Joyce, N.C. Transplantation of adult human corneal endothelium *ex vivo*: a morphologic study. *Cornea* **20**, 731, 2001.
- Mimura, T., Amano, S., Usui, T., Araie, M., Ono, K., Akihiro, H., Yokoo, S., and Yamagami, S. Transplantation of corneas reconstructed with cultured adult human corneal endothelial cells in nude rats. *Exp Eye Res* **79**, 231, 2004.
- Mimura, T., Yamagami, S., Yokoo, S., Usui, T., Tanaka, K., Hattori, S., Irie, S., Miyata, K., Araie, M., and Amano, S. Cultured human corneal endothelial cell transplantation with a collagen sheet in a rabbit model. *Invest Ophthalmol Vis Sci* **45**, 2992, 2004.
- Ishino, Y., Sano, Y., Nakamura, T., Connon, C.J., Rigby, H., Fullwood, N.J., and Kinoshita, S. Amniotic membrane as a carrier for cultivated human corneal endothelial cell transplantation. *Invest Ophthalmol Vis Sci* **45**, 800, 2004.
- Miyata, K., Drake, J., Osakabe, Y., Hosokawa, Y., Hwang, D., Soya, K., Oshika, T., and Amano, S. Effect of donor age on morphologic variation of cultured human corneal endothelial cells. *Cornea* **20**, 59, 2001.
- Mimura, T., and Joyce, N.C. Replication competence and senescence in central and peripheral human corneal endothelium. *Invest Ophthalmol Vis Sci* **47**, 1387, 2006.
- Kim, N.W., Piatyszek, M.A., Prowse, K.R., Harley, C.B., West, M.D., Ho, P.L., Coviello, G.M., Wright, W.E., Weinrich, S.L., and Shay, J.W. Specific association of human telomerase activity with immortal cells and cancer. *Science* **266**, 2011, 1994.
- Wang, X., Tsao, S.W., Wong, Y.C., and Cheung, A.L. Induction of senescent-like growth arrest as a new target in anticancer treatment. *Curr Cancer Drug Targets* **3**, 153, 2003.
- McGowan, S.L., Edelhauser, H.F., Pfister, R.R., and Whikehart, D.R. Stem cell markers in the human posterior limbus and corneal endothelium of unwounded and wounded corneas. *Mol Vis* **13**, 1984, 2007.

36. Whitehart, D.R., Parikh, C.H., Vaughn, A.V., Mishler, K., and Edelhauser, H.F. Evidence suggesting the existence of stem cells for the human corneal endothelium. *Mol Vis* **11**, 816, 2005.
37. Chiu, C.P., Dragowska, W., Kim, N.W., Vaziri, H., Yui, J., Thomas, T.E., Harley, C.B., and Lansdorf, P.M. Differential expression of telomerase activity in hematopoietic progenitors from adult human bone marrow. *Stem Cells* **14**, 239, 1996.
38. Zimmermann, S., Glaser, S., Ketteler, R., Waller, C.F., Klingmüller, U., and Martens, U.M. Effects of telomerase modulation in human hematopoietic progenitor cells. *Stem Cells* **22**, 741, 2004.
39. Hiyama, K., Hirai, Y., Kyoizumi, S., Akiyama, M., Hiyama, E., Piatyszek, M.A., Shay, J.W., Ishioka, S., and Yamakido, M. Activation of telomerase in human lymphocytes and hematopoietic progenitor cells. *J Immunol* **155**, 3711, 1995.
40. Konomi, K., and Joyce, N.C. Age and topographical comparison of telomere lengths in human corneal endothelial cells. *Mol Vis* **13**, 1251, 2007.
41. Allsopp, R.C., Vaziri, H., Patterson, C., Goldstein, S., Younglai, E.V., Futcher, A.B., Greider, C.W., and Harley, C.B. Telomere length predicts replicative capacity of human fibroblasts. *Proc Natl Acad Sci USA* **89**, 10114, 1992.
42. Simonsen, J.L., Rosada, C., Serakinci, N., Justesen, J., Stenderup, K., Rattan, S.I., Jensen, T.G., and Kassem, M. Telomerase expression extends the proliferative life-span and maintains the osteogenic potential of human bone marrow stromal cells. *Nat Biotechnol* **20**, 592, 2002.
43. Wang, J.C., Warner, J.K., Erdmann, N., Lansdorf, P.M., Harrington, L., and Dick, J.E. Dissociation of telomerase activity and telomere length maintenance in primitive human hematopoietic cells. *Proc Natl Acad Sci USA* **102**, 14398, 2005.
44. Zhu, C., and Joyce, N.C. Proliferative response of corneal endothelial cells from young and older donors. *Invest Ophthalmol Vis Sci* **45**, 1743, 2004.
45. Joyce, N.C., and Zhu, C.C. Human corneal endothelial cell proliferation: potential for use in regenerative medicine. *Cornea* **23**, S8, 2004.

Address correspondence to:

Satoru Yamagami, M.D.

Department of Ophthalmology

Tokyo Women's Medical University Medical Center East

Nishiogu 2-1-10, Arakawa-ku

Tokyo 116-8567

Japan

E-mail: syamagami-tky@umin.ac.jp

Received: September 9, 2009

Accepted: October 23, 2009

Online Publication Date: December 8, 2009



